DOE/MC/26015--2988

DE91 002068

Development of Improved Cathodes for Solid Oxide Fuel Cells

Final Report

H.U. Anderson

Work Performed Under Contract No.: DE-FG21-89MC26015

For
U.S. Department of Energy
Office of Fossil Energy
Morgantown Energy Technology Center
P.O. Box 880
Morgantown, West Virginia 26507-0880

By
University of Missouri-Rolla
211 Parker Hall
Rolla, Missouri 65401

March 1991

ABSTRACT

Objectives

The University of Missouri-Rolla conducted a 17 month research program focussed on the development and evaluation of improved cathode materials for solid oxide fuel cells (SOFC). The objectives of this program were:

- The development of cathode materials of improved stability in reducing environments.
- The development of cathode materials with improved electrical conductivity.

The program was successful in identifiying some potential candidate materials: Air sinterable $(La,Ca)(Cr,Co)O_3$ compositions were developed and found to be more stable than $La_{.8}Sr_{.2}MnO_3$ towards reduction. Their conductivity at 1000°C ranged between 30 to 60 S/cm. Compositions within the $(Y,Ca)(Cr,Co,Mn)O_3$ system were developed and found to have higher electrical conductivity than $La_{.8}Sr_{.2}MnO_3$ and preliminary results suggest that their stability towards reduction is superior.

TABLE OF CONTENTS

1. Introduction

Background Statements

The purpose of this project is to develop an improved cathode for high temperature fuel cells than is currently being employed.

This project is based on the need for a more stable and reliable cathode than is currently being employed in high temperature solid oxide fuel cells (SOFC). The inability of the $LaMnO_3$ based cathodes to withstand exposure to fuel gas without degrading their performance is one of the foremost problems confronting the successful commercialization of SOFC's.

As part of our DOE-BES program we have been investigating a number of conducting perovskite systems. Recent results indicate that some of the compositions in these systems possess electrical conductivity and stability towards reduction superior to the currently used SOFC cathode, $La_{.8}Sr_{.2}MnO_3$. These results are very encouraging and suggest that we have the ability to develop an improved cathode for SOFC's. In this program we are expanding our DOE-BES studies with the intent of developing a composition which will out-perform $La_{.8}Sr_{.2}MnO_3$ as a SOFC cathode.

In our DOE-BES program we have shown that the system $La_{1-x}Ca_xCr_{1-y}Co_yO_3$ (x = 0.1-0.3 and y = 0.1-1.0) can be sintered to densities > 95% TD in air at 1400°C and below. The electrical conductivity (d.c.) measurements were made as a function of temperature and in the oxygen activity range from 1 to 10^{-19} atm. Details of the Apparatus and experimental setup are explained elsewhere.(1) At 1000°C and 1 atm. the conductivity ranges from 17 S/cm to 58 S/cm for $La_{.9}Ca_{.1}Cr_{.9}Co_{.1}O_3$ and $La_{.7}Ca_{.3}Cr_{.8}Co_{.2}O_3$, respectively. Stability studies were done by quenching powder samples from 1000°C and 10^{-19} atm. and subjecting quenched powders to X-ray diffraction. X-ray diffraction patterns of reduced samples for y = 0.1, 0.2 and 0.3 showed no second phase indicating that these compositions are structurally stable throughout the entire temperature and oxygen activity range studied.

The observed results on sintering, electrical conductivity and stability towards reduction demonstrate that $LaCrO_3$ can be sintered in air at 1400°C and below with varying the composition without the deterioration of either the electrical conductivity nor high temperature stability of the resulting dense ceramics.

2. Project Description

The past DOE sponsored program has permitted the principal investigators to acquire valuable information regarding the stability of perovskite type structures towards oxidation and reduction at elevated temperatures. Through these studies a substantial base of knowledge and research capabilities was established, thus tailored materials with the desired properties can be developed. The principal investigators are using this unique background as the basis to address the problem of:

- development of a cathode material which is more stable towards reduction than the state-of-the-art Sr-doped $LaMnO_3$ that is currently used.
- development of a cathode material which has higher electrical conductivity than Sr doped $LaMnO_3$, i.e. > 100 S/cm at 1000°C.

The systems targeted for this study are: $(La,Ca)(Cr,Co)O_3$ and $(Y,Ca)(Cr,Mn,Co)O_3$. These systems were chosen because of our previous knowledge and the fact that substantial mutual solubility exists for both systems. A series of compositions in the $LaCrO_3$-$LaCoO_3$-CaO, CaO-$LaMnO_3$, $YCrO_3$-$YMnO_3$-$YCoO_3$-CaO, and CaO-$YMnO_3$ systems were synthesized using the organometallic preparation technique.[2] The resulting powders were milled and subjected to X-ray diffraction to ensure that they were single phase. For the electrical conductivity and sintering studies the powders were pressed into bars with the aid of polyvinyl alcohol and water binder. A compaction pressure of 1500-2500 kg/cm^2 yielded 0.6x0.4x3.0 cm^3 bars with green density of about 45-52% of theoretical. Densification was carried out over the temperature range 1100 to 1500°C for 2 to 10 hours in a SiC heated furnace. Bulk densities were measured by the liquid (Freon) displacement technique. Scanning electron micrographs of the polished and thermally etched surfaces of sintered specimens were taken using a JEOL JSM-35 CF scanning electron microscope.

Electrical conductivity and thermoelectric power measurements were made simultaneously in an apparatus which could measure three samples at a time. For these measurements the samples were cut into bars with the dimensions (0.3x0.3x2.0 cm^3) and electroded with Pt paste. The specimens were mounted between two platinum blocks, which had Pt-10% Rh/Pt thermocouples as electrical contacts, Pt wire heater was welded on the lower end of the holder to generate the temperature gradient along the vertical direction. Three sets of specimens and holders were contained in Al_2O_3 tubes within a $MoSi_2$ furnace, where the temperature was controlled by a Eurotherm temperature controller. The oxygen activity over the samples was controlled by using flowing gas mixtures of either O_2 -N_2 or CO_2-forming gas ($10H_2$-$90N_2$). A stabilized zirconia oxygen sensor was used to monitor the

oxygen partial pressure of the gas mixture. The Seebeck coefficients were determined by measuring temperature gradients and thermal emf's through the common leads of the thermocouples. Electrical conductivity measurements were made using the two-probe, four-wire Kelvin technique in which two leads carry the test signal (1mA) and the other two measure the voltage drop. The measurements were made using a data logger (a Hewlett Packard 3497A data acquisition/control unit), which employs a HP-85 computer both as a control and readout device. Thermal expansion measurements were made on an Orton dilatometer over the temperature range 25 to 1000°C.

3. Results and Discussion

I. Sintering Studies

The primary difficulty of sintering $LaCrO_3$ and $YCrO_3$ based perovskites in air arises from the volatilization of Cr from the structure at temperatures in excess of 1400°C, resulting in porosity. This is inhibited by using reducing atmospheres during sintering, with oxygen activities of 10^{-10}-10^{-12} at 1700°C.[2] Meadowcroft[4] showed that the sintered density of $La_{.84}Sr_{.16}CrO_3$ increased when excess Sr was added in the form of $SrCO_3$ before sintering. The maximum beneficial effect observed was a sharp increase in sintered density when 4 m% $SrCO_3$ was added. This was probably due to the formation of $SrCrO_4$ at intermediate temperatures followed by melting and liquid-phase sintering. Flandermeyer et.al.[4] used low melting oxide eutectics as well as La, Y and Mg fluorides up to 8-10 wt% to increase the density of sintered compacts, however, these fluxes are not desirable in the SOFC environment (1000°C). In this study, we have incorporated various dopants, on both La and Cr sites of the $LaCrO_3$ and $YCrO_3$ compounds, to enhance the sinterability in air. These dopants, Ca and Co, are expected to generate a transient liquid to aid sinterability in air at temperatures below 1400°C.

A. $(La,Ca)(Cr,Co)O_3$ System

In the case of $LaCrO_3$, neither Ca nor Co additions by themselves enhanced sinterability when added at levels of less than 30 m% (see Table I).

These results show that the substitution of Co for Cr in $LaCrO_3$ improved the sinterability. Significant improvement in densification was observed with substitution of 20 m% Co for Cr, and 95% theoretical density was achieved in air at 1500°C with substitution of 50 m% Co for Cr. However, substitution of Ca for La in $LaCrO_3$ did not improve the

sinterability, but in $LaCoO_3$ sinterability was improved and the melting temperature was reduced. The Co substitution for Cr in $LaCrO_3$ apparently forms a hitherto unidentified transient liquid in air at temperatures below 1500°C, thereby improving sinterability. However, when both Ca and Co are added simultaneously, sintering occurred at temperatures below 1450°C (see Table II).

Table I. Sintered Density and Percent Theoretical Density as a Function of Co and Temperature. (Sintering Time 2 hrs.)

$LaCr_{1-y}Co_yO_3$ Composition (y)	Temperature (°C) 1100 Density g/cc	%TD	1200 Density g/cc	%TD	1300 Density g/cc	%TD	1400 Density g/cc	%TD	1500 Density g/cc	%TD
y = 0.0	4.06	60	4.08	61	4.09	61	4.10	61	4.11	61
y = 0.1	4.32	64	4.33	64	4.35	64	4.41	65	4.62	68
y = 0.2	4.80	70	4.93	73	5.23	77	5.50	81	5.73	85
y = 0.5	5.05	72	5.22	75	5.73	82	6.08	87	6.63	95
y = 0.7	5.15	73	5.42	77	5.95	84	6.21	88	MELTED	
y = 1.0	5.88	82	6.06	84	6.27	94	6.42	95	MELTED	

Table II. Sintered Density and Percent Theoretical Density as a Function of Ca and Temperature. (Sintering Time 2 hrs.)

$La_{1-x}Ca_xCr_{0.9}Co_{0.1}O_3$ Composition (x)	Temperature (°C) 1100 Density g/cc	%TD	1200 Density g/cc	%TD	1300 Density g/cc	%TD	1400 Density g/cc	%TD	1500 Density g/cc	%TD
x = 0.0	4.32	64	4.33	64	4.35	64	4.41	65	4.62	68
x = 0.1	4.52	68	4.60	70	5.37	81	5.92	90	6.34	96
x = 0.2	4.82	74	5.13	79	5.87	90	6.11	94	6.22	96
x = 0.3	5.34	83	5.74	89	5.96	93	6.09	95	6.10	95
$La_{0.7}Ca_{0.3}CrO_3$	3.80	62	3.87	62	3.90	63	3.92	63	4.16	68
$La_{0.7}Ca_{0.3}CoO_3$	5.66	89	6.09	95	MELTED					

The enhancement of sintering is due to the formation of a CaO/CoO liquid phase at temperatures below 1300°C. Figure 1 is a SEM photomicrograph of a polished surface from a specimen of composition $La_{.8}Ca_{.2}Cr_{.8}Co_{.2}O_3$ which was sintered for only ten minutes at 1200°C and quenched. As can be seen much liquid (glassy-like phase) was present.

In summary, we were sucessful in developing $La_{1-x}Ca_xCr_{1-y}Co_yO_3$ compositions that sintered at temperatures below 1400°C in air with the aid of liquid phase. The composition of the liquid phase was dependent upon the amount of Co and Ca substitution. The liquid phase dispersed along the grain boundaries and did not alter the electrical conductivity and stability of the materials if the Co substitution for Cr was kept lower than 30 m%; otherwise, the stability against reduction at high temperature was diminished.

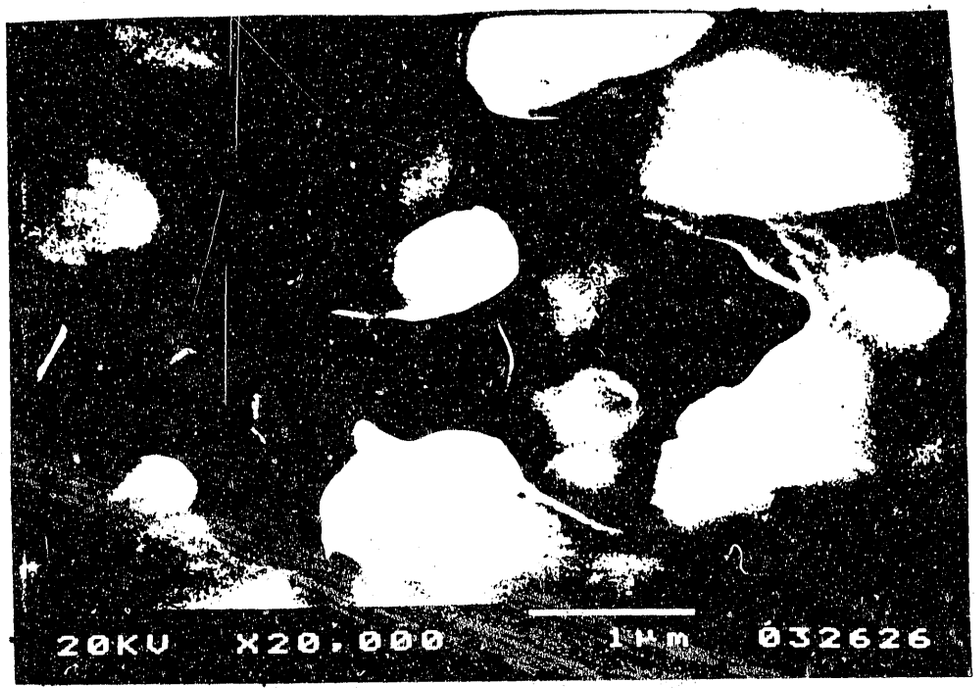

Figure 1: **$La_{.8}Ca_{.2}Cr_{.8}Co_{.2}O_3$ heated at 1200°C for 10 Min. and water quenched to room temperature**

B. <u>$(Y,Ca)(Cr,Mn,Co)O_3$ System</u>

Calcium is soluble in $YCrO_3$ up to 20 m% with no change in the orthorhombic crystal structure.

$Y_{1-x}Ca_xCrO_3$ is difficult to densify. It requires temperatures of 1750°C and oxygen activity of less than 10^{-9} atm similar to $LaCrO_3$. However, these compositions are found to be stable towards reduction in H_2 at temperatures to 1500°C. $Y_{1-x}Ca_xMnO_3$ has a miscibility gap for 10 m% < Ca < 40 m% (see Table III). For Ca < 10 m%, the crystal structure is hexagonal and for Ca > 40 m% it becomes orthorhombic. Pure $YMnO_3$ is difficult to densify, however, compositions containing more than 30 m% Ca densify well at 1400°C.

Table III. Conductivity and TEC of $Y_{1-x}Ca_xMnO_3$ as a function of Ca content

Ca Content	TEC (500-1000°C)	σ(900°C)	Structure
0 m%	$11.5 \times 10^{-6}C^{-1}$	0.2 S/cm	Hex
10	10.0	13	Hex/Ortho
20	9.7	52	Hex/Ortho
30	9.7	85	Hex/Ortho
40	10.1	133	Ortho
50	8.5	190	Ortho

In an effort to densify $YCrO_3$ in air we have tried the same procedure used for $LaCrO_3$. That is, the simultaneous substitution of Ca and Co. Our initial results indicate that this system can be densified in air at temperatures below 1500°C. Summary of our results was presented at the 1990 Fuel Cell Seminar in Phoenix, AZ in November 1990.

II. Electrical Conductivity Studies

A. $LaCrO_3$ System

D.C. electrical conductivity measurements were made for compositions in air over a temperature range from 20 to 1200°C. Previous studies on $(La,Ca,Sr)CrO_3$[6,7] and $(La,Ca,Sr)CoO_3$[8-13] show both systems to be p-type conductors with holes moving through the structure by the small polaron mechanism.

The electrical conductivity for small polarons takes the form:

$$\sigma = (C/T) \exp(-E/kT) \quad (1)$$

where C is both a charge carrier concentration and material constant, T is the absolute temperature, E is activation energy and k is Boltzman's constant. Therefore, for materials which obey the small polaron mechanism, a plot of log (σT) versus 1/T gives a straight line whose slope is proportional to the activation energy. Charge is transferred when the polaron hops from one cation to another. The electrical conductivity is often enhanced by substituting a lower valence ion (acceptor) such as Ca for La.

The electrical conductivity data for $La_{1-x}Ca_xCr_{0.9}Co_{0.1}O_3$, $La_{1-x}Ca_xCr_{0.8}Co_{0.2}O_3$ and $La_{1-x}Ca_xCr_{0.7}Co_{0.3}O_3$ (with x=0.1, 0.2 and 0.3) are shown in figures 2, 3, and 4, respectively, as log (σ) versus reciprocal temperature. When plotted as log σT versus reciprocal temperature, the plots are linear suggesting that the small polaron mechansim is obeyed. For a given Ca content, the activation energies were independent of Co concentration, the

approximate values were 0.45, 0.2, 0.2 and 0.2 ev for Ca contents of 0, 10, 20 and 20 mole % respectively.

Previous studies on $(La,Ca)CrO_3$[7] and $(La,Ca)CoO_3$[8] have shown that they have intrinsic p-type conductivity due to the formation of cation vacancies. The electrical conductivity in these oxides is enhanced by substituting Ca^{2+} for La^{3+}, which is compensated by a $Cr^{3+} \rightarrow Cr^{4+}$ transition. This can be represented, for Ca doped $LaCrO_3$, by:

$$La_{1-x}^{3+}Ca_x^{2+}Cr_{1-x}^{3+}Cr_x^{4+}O_3 \qquad (2)$$

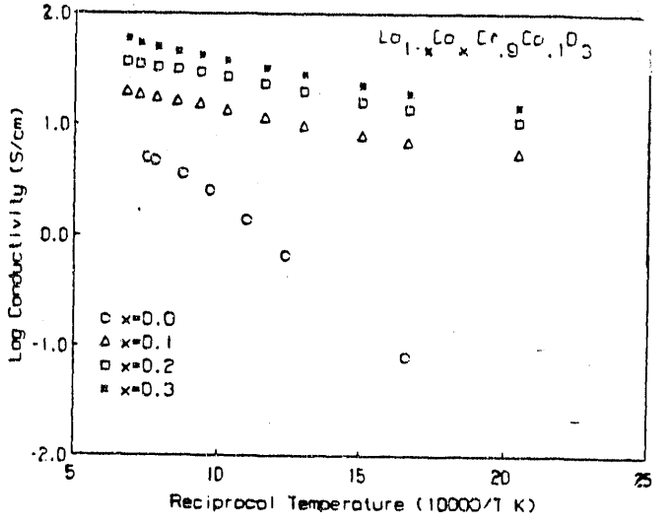

Figure 2: **Electrical conductivity of $La_{1-x}Ca_xCr_{.9}Co_{.1}O_3$ as a function of Ca content and temperature**

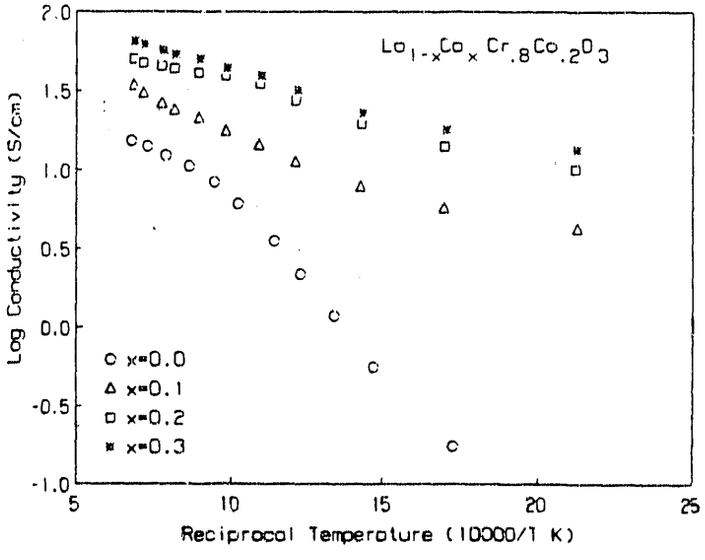

Figure 3: **Electrical conductivity of $La_{1-x}Ca_xCr_{.8}Co_{.2}O_3$ as a function of Ca content and temperature**

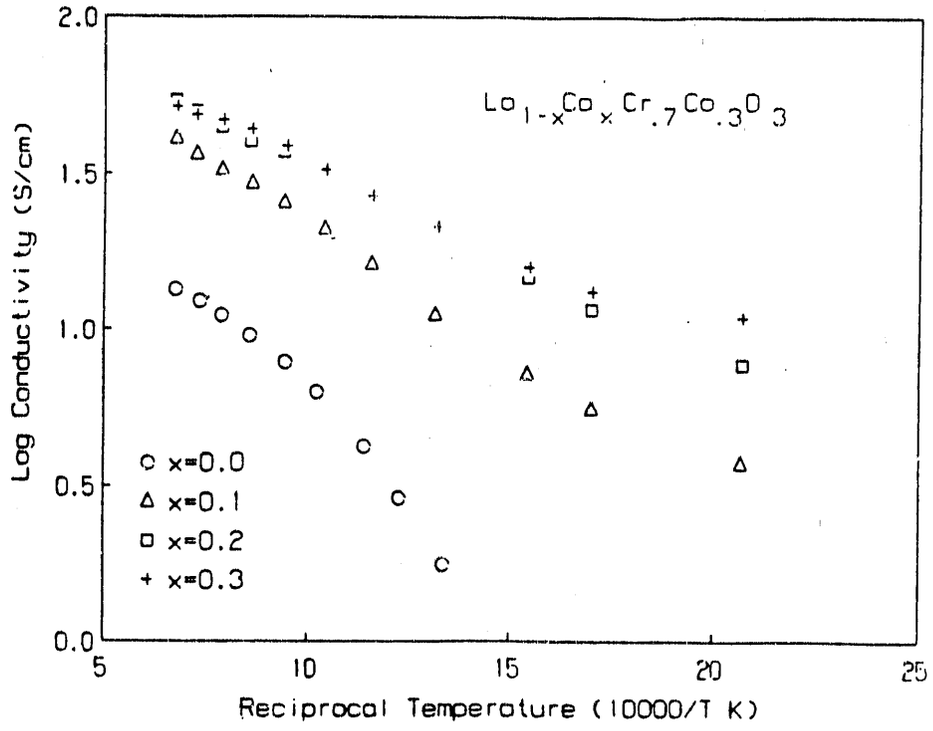

Figure 4: Electrical conductivity of $La_{1-x}Ca_xCr_{.7}Co_{.3}O_3$ as a function of Ca content and temperature

It is believed that the Cr^{3+} d states with t_{2g} symmetry have small overlap integrals resulting in narrow bands and a tendency toward localization, whereas d states with e_g symmetry have a larger overlap, due to hybridization with oxygen levels, and form a wider band of itinerant states higher in energy and not occupied in the ground state of the system. All levels associated with the A sublattice atoms are well above or below the Fermi energy, and their primary role is to determine the occupancy of the t_{2g} Cr states through charge compensation.[6] Substitution of Ca for La will create a hole in the Cr t_{2g} band and lead to an increase in the electrical conductivity.

As for Sr and Ba substitutions in $LaCoO_3$,[10,11] electrical neutrality of solid solutions of $La_{1-x}Ca_xCoO_3$ can be achieved either via the formation of Co^{4+} or by oxygen vacancies, $V_O^{\cdot\cdot}$, or both, following the equation:

$$La_{1-x}^{3+}Ca_x^{2+}Co^{3+}_{1-x+2y}Co^{4+}_{x-2y}O^{2-}_{3-y}(V_O^{\cdot\cdot})_y \quad (3)$$

The substitution of La^{3+} by Ca^{2+} in $LaCoO_3$ leads to an increase in the electrical conductivity and to a transformation from semiconductive to metallic conductivity.[12] No contribution to the electronic conductivity is anticipated if the substitution of La^{3+} by Ca^{2+} is compensated by the formation of oxygen vacancies.

As in the case of $La_{1-x}Ca_xCrO_3$ and $La_{1-x}Ca_xCoO_3$, the substitution of Ca for La in $La_{1-x}Ca_xCr_{1-y}Co_yO_3$, should result in the formation of Cr^{4+} and Co^{4+} in order to preserve the electrical neutrality. Figure 5 shows the electrical conductivity at 1000°C as a function of Ca

content in $La_{1-x}Ca_xCr_{0.9}Co_{0.1}O_3$ and $La_{1-x}Ca_xCr_{0.8}Co_{0.2}O_3$. The electrical conductivity at 1000°C as a function of Ca in $La_{1-x}Ca_xCrO_3$ is included from reference 6 for comparison and to provide a relative y = 0.0 case. As can be seen, the electrical conductivity of $La_{1-x}Ca_xCr_{0.9}Co_{0.1}O_3$ and $La_{1-x}Ca_xCr_{0.8}Co_{0.2}O_3$ at 1000°C is slightly higher than that of $La_{1-x}Ca_xCrO_3$. This may be due to a contribution of Co to the conductivity, but this is yet to be confirmed.

Seebeck measurements were made in order to determine the type and concentration of charge carriers. Figures 6-8 are the resulting Seebeck coefficients plotted as a function of temperature for $LaCr_{1-y}Co_yO_3$, $La_{1-x}Ca_xCr_{0.9}Co_{0.1}O_3$ and $La_{1-x}Ca_xCr_{0.8}Co_{0.2}O_3$, respectively. (In figure 8, the dashed line is taken from Ref. 6 for comparison.) In $LaCr_{1-y}Co_yO_3$, the substitution of Co for Cr increases the carrier concentration.

As the Ca content increased, the Seebeck coefficients exhibited a temperature independent behavior, indicating that the carrier mobility, rather than carrier concentration, was thermally activated. According to Heikes formula this type of behavior indicates a small polaron conduction mechanism which agrees with the electrical conductivity measurements.

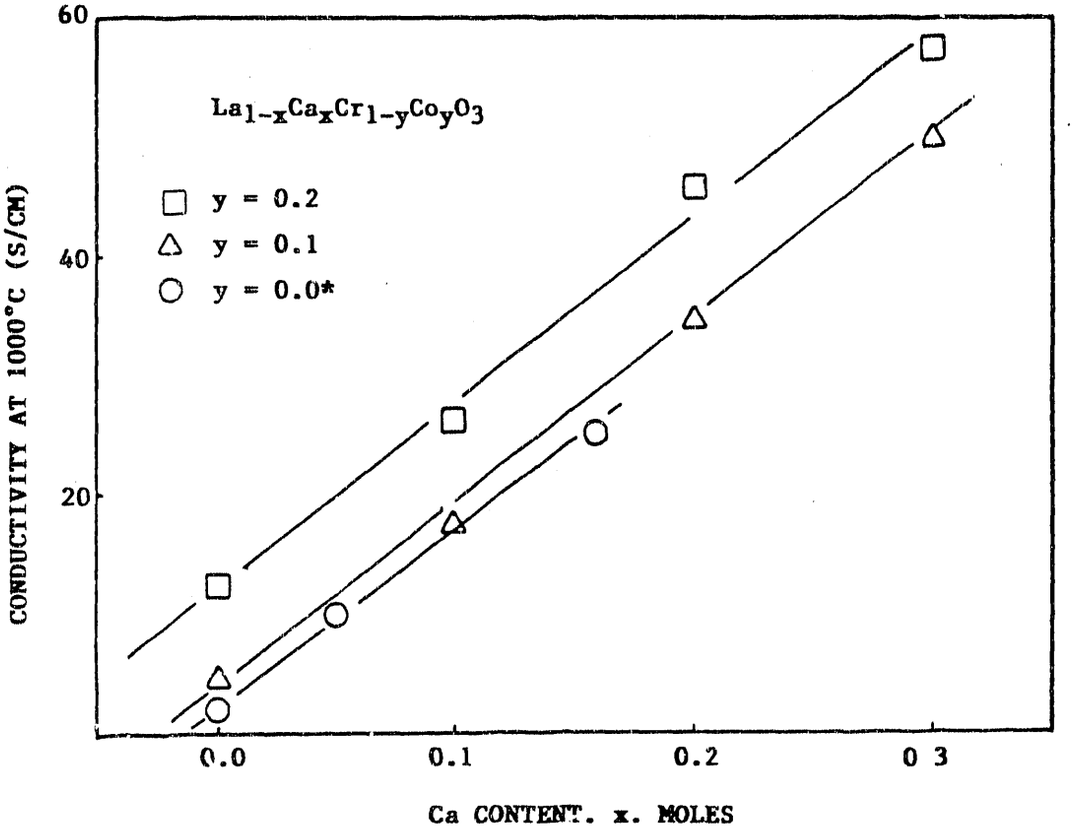

Figure 5: **Electrical conductivity at 1000°C as a function of Ca content**
***S. Song, et al.[7]**

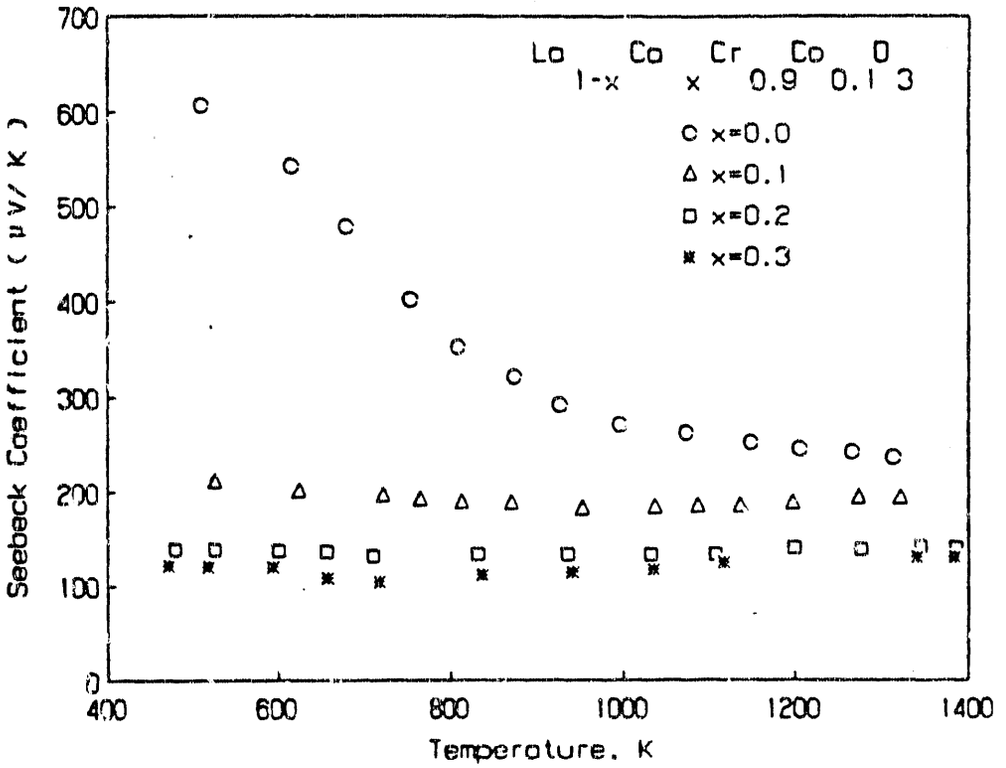

Figure 6: **Seebeck coefficients of $La_{1-x}Ca_xCr_{.9}Co_{.1}O_3$ as a function of Ca and temperature**

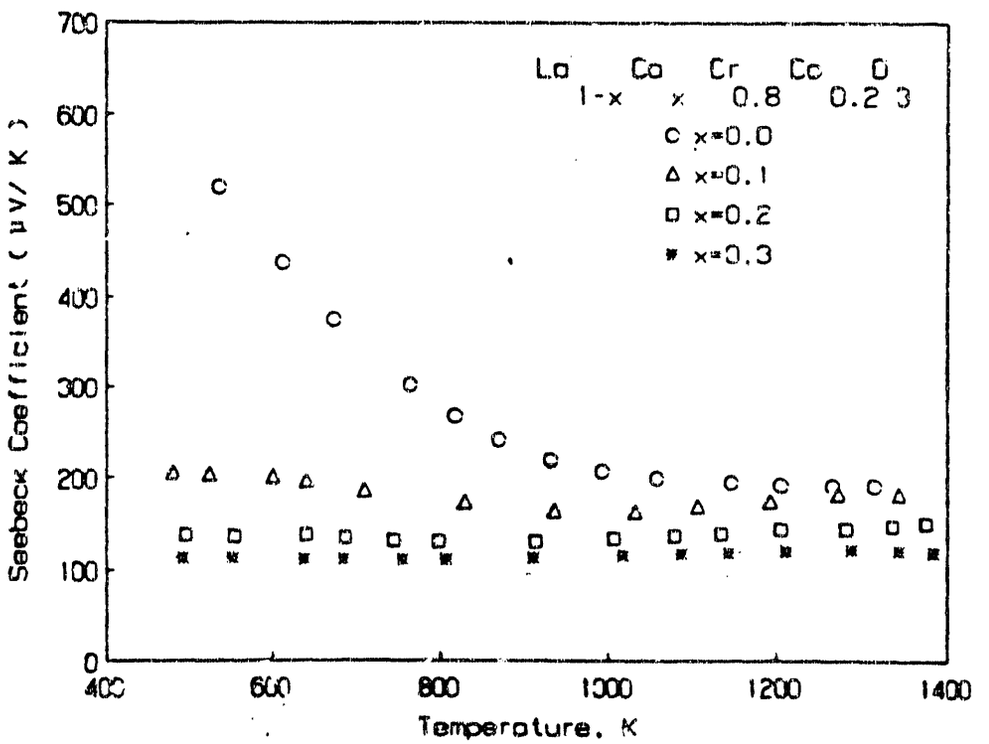

Figure 7: **Seebeck coefficients of $La_{1-x}Ca_xCr_{.8}Co_{.2}O_3$ as a function of Ca and temperature**

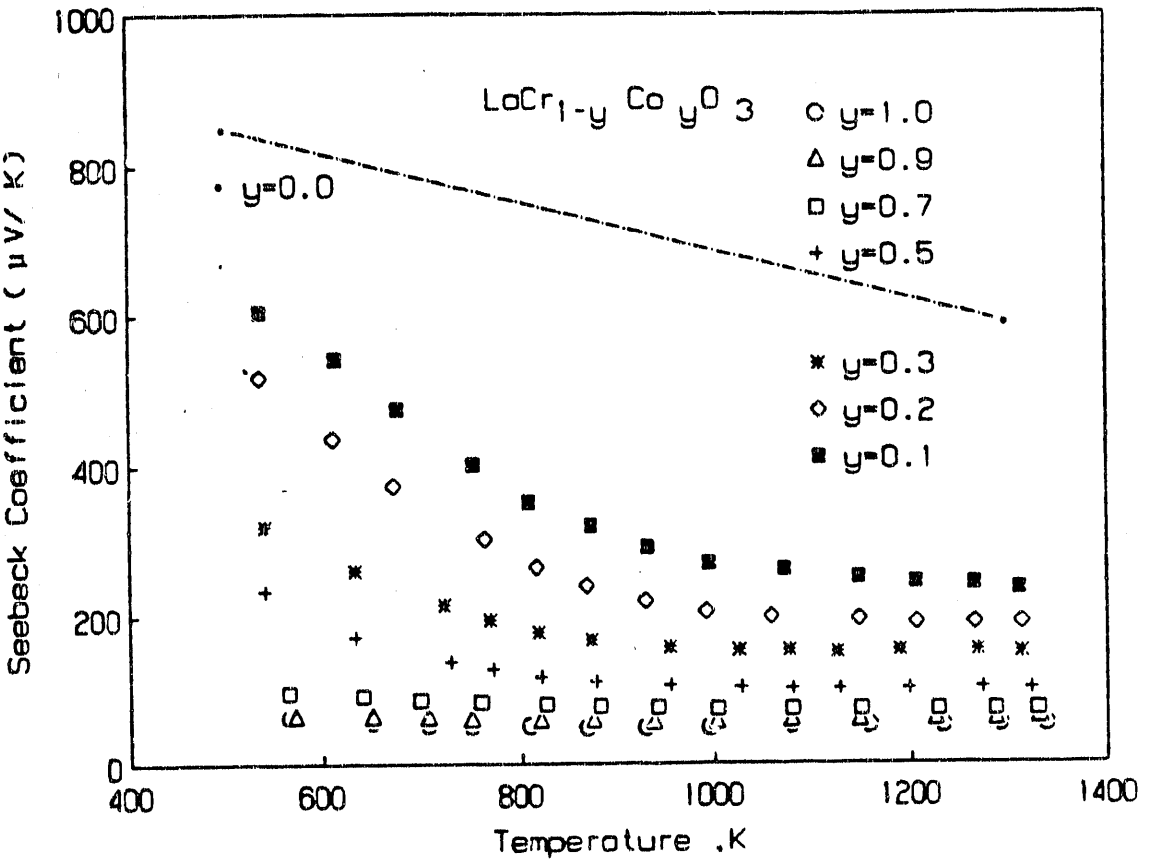

Figure 8: Seebeck coefficients of $LaCr_{1-y}Co_yO_3$ as a function of Co content and temperature

Oxygen Activity Dependence

The dc electrical conductivity measurements for $La_{1-x}Ca_xCr_{1-y}Co_yO_3$ (x = 0.1, 0.2, 0.3 and y = 0.1, 0.2, 0.3) were made as a function of oxygen activity at 1000°C. The results are shown in figures 9-10. The electrical conductivity data showed similar oxidation-reduction behavior. In the high oxygen activity region, within the experimental error, the electrical conductivity was nearly constant. The conductivity decreased as a function of oxygen activity to the one quarter power as reduction progressed. The constant electrical conductivity which exists in the high oxygen activity region may be easily understood if it is assumed that the carrier concentration and electronic compensation predominate. In the low oxygen activity region, oxygen vacancies are formed and the electrical conductivity begins to decrease as a result of ionic compensation.

From defect chemistry modeling, the defect structure and electrical conductivity changes can be predicted under various oxygen activity and temperature conditions. A model is adopted, based on that developed for Mg-doped $LaCrO_3$[14], to explain the electrical conductivity of $La_{1-x}Ca_xCr_{1-y}Co_yO_3$ (where y is less than 0.3) as a function of oxygen activity. In $La_{1-x}Ca_xCr_{1-y}Co_yO_3$, Co^{3+} substitutes for Cr^{3+}, and Ca^{2+} substitutes for La^{3+} on normal

lattice sites. The acceptor Ca^{2+} possesses one effective negative charge which can be compensated for either by $Cr^{3+} \rightarrow Cr^{4+}$ or $Co^{3+} \rightarrow Co^{4+}$ transitions or by the formation of oxygen vacancies. If such a substitution is compensated by the formation of oxygen vacancies, no contribution to the electronic conductivity is anticipated.

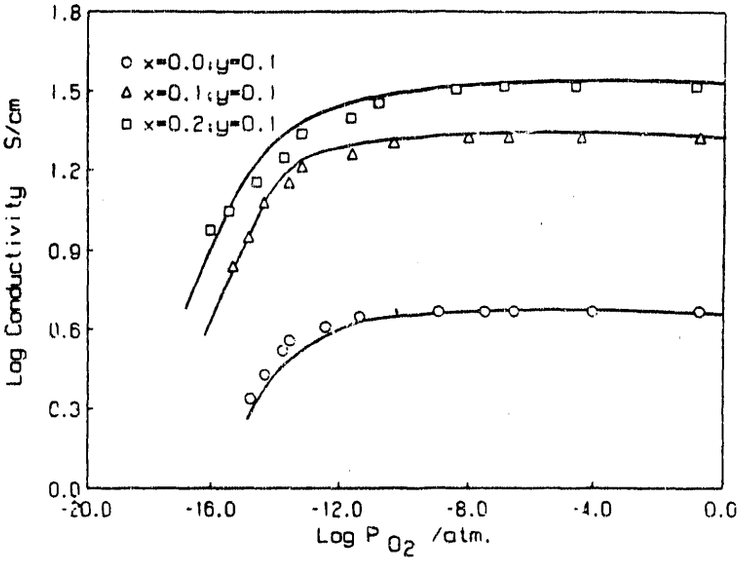

Figure 9: **Log conductivity vs. log oxygen activity for $La_{1-x}Ca_xCr_{.9}Co_{.1}Co_3$ at 1000°C (Solid lines were derived from the model)**

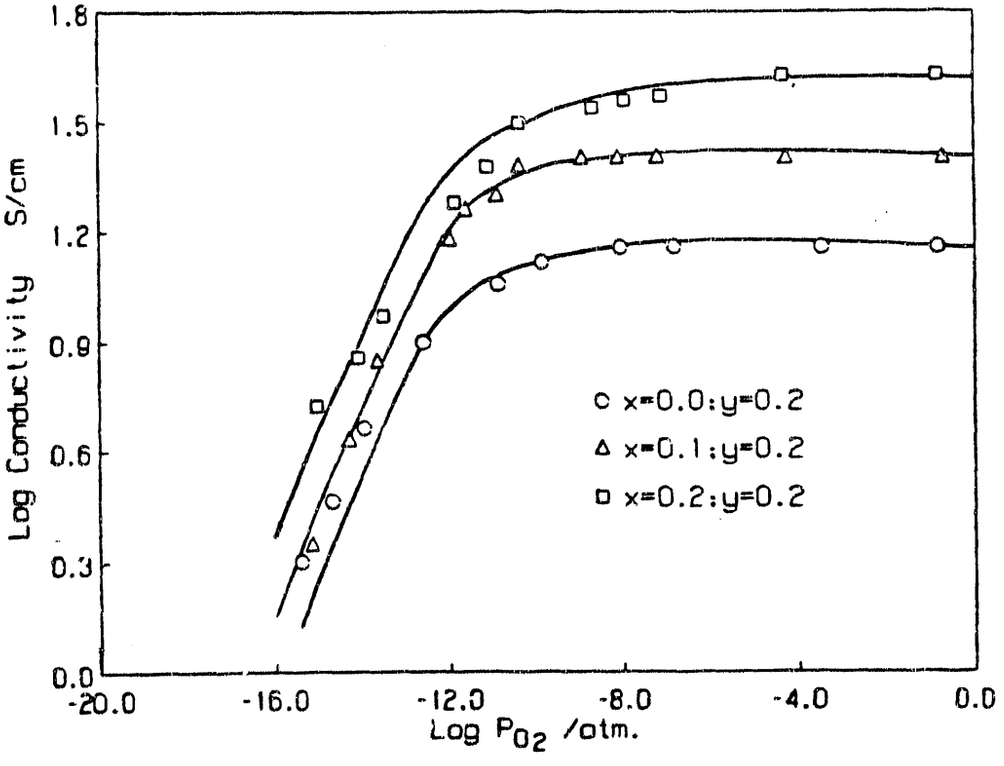

Figure 10: **Log conductivity vs. log oxygen activity for $La_{1-x}Ca_xCr_{.8}Co_{.2}O_3$ at 1000°C (Solid lines were derived from the model)**

Since, for this compound, the cations and anions are of comparable size, it can be assumed that the native defects are of the Schottky type. The Schottky reaction, using the Kroger-Vink notation[15], is expressed by

$$nill = V'''_{La} + V'''_{Cr,Co} + V^{\cdot\cdot}_{O} \quad (4)$$

$$K_s = [V'''_{La}]\,[V'''_{Cr,Co}]\,[V^{\cdot\cdot}_{O}]^3 \quad (5)$$

Since this is a closed system, the cation stoichiometry must remain constant, therefore, $[V'''_{La}] = [V'''_{Cr,Co}] = 2[V'''_{M}]$ throughout the entire single-phase region.

$$K_s = [V'''_{M}]^2\,[V^{\cdot\cdot}_{O}]^3 \quad (6)$$

The p-type nonstoichiometric reaction is given by

$$3/2\ O_2 = V'''_{La} + V'''_{Cr,Co} + 6h^{\cdot} + 3O_O \quad (7)$$

$$K_8 = [V'''_{M}]^2\,p^6\,P_{O2}^{-3/2} \quad (8)$$

When Ca^{2+} is substituted for La^{3+}, the Ca^{2+} will possess one effective negative charge which can be compensated either by a $B^{3+} \rightarrow B^{4+}$ transition or by the formation of oxygen vacancies. This leads to the following overall electrical neutrality condition

$$2\,[V^{\cdot\cdot}_{O}] + p = 6\,[V'''_{M}] + [Ca'_{M}] \quad (9)$$

At high oxygen activity, electronic compensation is expected and assuming that both $[V^{\cdot\cdot}_{O}]$ and $[V'''_{M}]$ are smaller than the impurity content, the neutrality condition becomes

$$p = [Ca'_{M}] \quad (10)$$

and from Eqs. 7 and 9

$$[V'''_{M}] = K_8^{1/2} P_{O2}^{3/4} / [Ca'_{M}] \quad (11)$$

$$[V^{\cdot\cdot}_{O}] = K_s^{1/3}\,[Ca'_{M}]\,P_{O2}^{-1/2} / K_8^{1/3} \quad (12)$$

respectively.

At low oxygen activities, oxygen may be lost and ionic compensation takes place through the formation of oxygen vacancies. In this case the electrical neutrality condition becomes

$$p = [Ca'_{M}] - 2\,[V^{\cdot\cdot}_{O}] \quad (13)$$

This condition can be expressed by

$$La_{1-y}Ca'_{y}M^{x}_{1-y}M^{\cdot}_{y}O_3 = La_{1-y}Ca'_{y}M^{x}_{1-y+2x}M^{\cdot}_{y-2x}V^{\cdot\cdot}_{ox}O_{3-x} + x/2\ O_2$$

or simply by

$$O_O + 2M^{\cdot}_{M} = 2M^{x}_{M} + V^{\cdot\cdot}_{O} + 1/2\ O_2 \quad (14)$$

where y is the amount of dopant and x is the concentration of oxygen vacancies. The equilibrium constant for reaction 14 can be expressed as

$$K_{14} = [M^{x}_{M}]^2\,[V^{\cdot\cdot}_{O}]\,P_{O2}^{1/2} / [M^{\cdot}_{M}]^2 \quad (15)$$

which in terms of mole fraction becomes

$$K_{14} = (1\text{-}y + 2x)^2 \times P_{O2}^{1/2} / (y\text{-}2x)^2 \quad (16)$$

Eq. 16 can be solved to yield

$$2x = y - \{P_{O2}^{1/2} (8\, y\, K_{14} P_{O2}^{-1/2} + 1)^{1/2} - 1)/4\, K_{14}\} \quad (17)$$

Since the electrical conductivity for p-type materials is given by

$$\sigma = e\, p\, \mu \quad (18)$$

where e is the electron charge, μ is the mobility, and p is the concentration of carriers which, from the model, is equal to y-2x. Thus, Eq. 18 can be rearranged to give

$$\sigma = e\, P_{O2}^{1/2} \mu((8\, y\, K_{14} P_{O2}^{-1/2} + 1)^{1/2} - 1)/4\, K_{14} \quad (19)$$

At the high oxygen activity region, Eq. 17 reduces to x = 0 and Eq. 19 reduces to $\sigma = e\mu y$, whereas in the low oxygen activity region the respective equations are reduced to

$$p = (y\text{-}2x)/y = P_{O2}^{1/4} / (2yK_{14})^{1/2} \quad (20)$$

or

$$\sigma = (e\mu y^{1/2} P_{O2}^{1/4}) / 2K_{14} \quad (21)$$

and

$$\sigma / \sigma_R = P_{O2}^{1/4} / (2\, y\, K_{14})^{1/2} \quad (22)$$

where σ_R is the electrical conductivity at 1 atm. oxygen.

The equilibrium constant K_{14} can thus be calculated by combining the electrical conductivity experimental data and Eq. 22. Theoretical curves can be generated by using Eq. 22 and the calculated values of K_{14}. The individual symbols in figures 9-10 represent the experimental data while the lines are the calculated curves from the model. At high oxygen activity the electrical conductivity was independent of the oxygen activity due to the expected electronic compensation. At low oxygen activity the electrical conductivity exhibited a 1/4 power dependence on the oxygen activity. The switch from P_{O2} independent to P_{O2} dependent region occurred at $\sim 10^{-10}$ atmos at 1000°C.

The stability of $La_{1-x}Ca_xCr_{1-y}Co_yO_3$ towards reduction is compared to that of $La_{1-x}Sr_xMnO_3$ and $LaCr_{1-x}Mg_xO_3$ in Table IV and figure 11. Ca and Co doping significantly increased the conductivity of $LaCrO_3$ and extended its stability to lower oxygen activity. The compositions $La_{1-x}Ca_xCr_{1-y}Co_yO_3$ with x = 0.0-0.3 and y = 0.1-0.2 are found to be stable toward dissociation in forming gas at 1000°C even though the electrical conductivity does decrease because of the low oxygen activity ($P_{O2} \simeq 10^{-16}$ atmos).

Table IV. **Electrical Conductivity of $La_{.8}Sr_{.2}MnO_3$, $LaCr_{.95}Mg_{.05}O_3$ and $La_{.8}Ca_{.2}Cr_{.9}Co_{.1}O_3$ as Function of Oxygen Activity at 1000°C.**

P_{O2} (atm.)	$La_{.8}Sr_{.2}MnO_3$ σ (S/cm)	$LaCr_{.95}Mg_{.05}O_3$ σ (S/cm)	$La_{.8}Ca_{.2}Cr_{.9}Co_{.1}O_3$ σ (S/cm)
10^{0}	150	3.2	34
10^{-8}	150	3.2	34
10^{-10}	125	3.2	30
10^{-12}	65	3.2	25
10^{-14}	22 (dissociated)	2.5 (stable)	16 (stable)
10^{-16}	10 (dissociated)	0.32 (stable)	9 (stable)

The electrical conductivities were found to be inversely proportional to the Seebeck coefficients throughout the entire oxygen activity range. The Seebeck coefficient increased and the electrical conductivity decreased with decreasing oxygen activity. This is true for all the regions of oxygen excess, stoichiometry and oxygen deficiency. Since the investigated compounds were stable under reducing conditions as well as oxidizing conditions, no degradation was observed on the Seebeck measurements at 1000°C, contrary to our observations on the $LaMnO_3$ based perovskite oxides[14]. These findings are very encouraging and should be investigated further, inorder to identify the parameters that increase the conductivity while maintaining the stability of $LaCrO_3$.

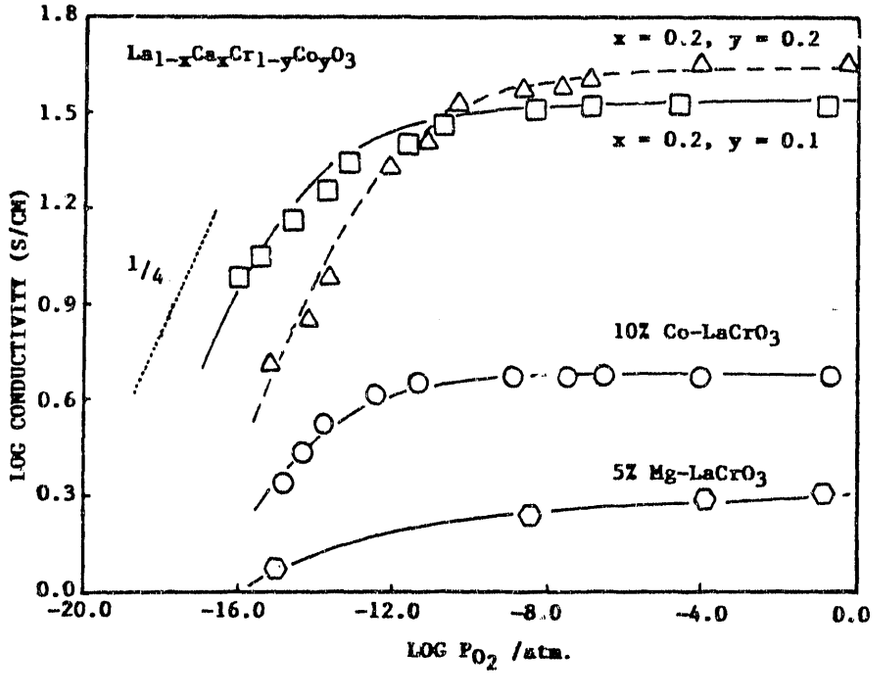

Figure 11: **Log conductivity vs. log oxygen activity for doped $LaCrO_3$ at 1000°C (Solid lines were derived from the model)**

B. $YCrO_3$ - $YMnO_3$ System

The electrical conductivity of $Y_{1-x}Ca_xCrO_3$ was studied both as function of Ca content and oxygen activity. At 1000°C, the maximum conductivity in air was 16 S/cm.

Examples of the electrical conductivity data are contained in figures 12, 13 and 14. The same model can be used to explain these data as that for $LaCrO_3$ so will not be reproduced here.

A comparison between the reduction characteristics of $YCrO_3$, $LaCrO_3$ and $LaMnO_3$ were made and we found that $Y_{.8}Ca_{.2}CrO_3$ is more stable towards reduction than either Sr doped $LaMnO_3$ or $LaCrO_3$. (See figure 15)

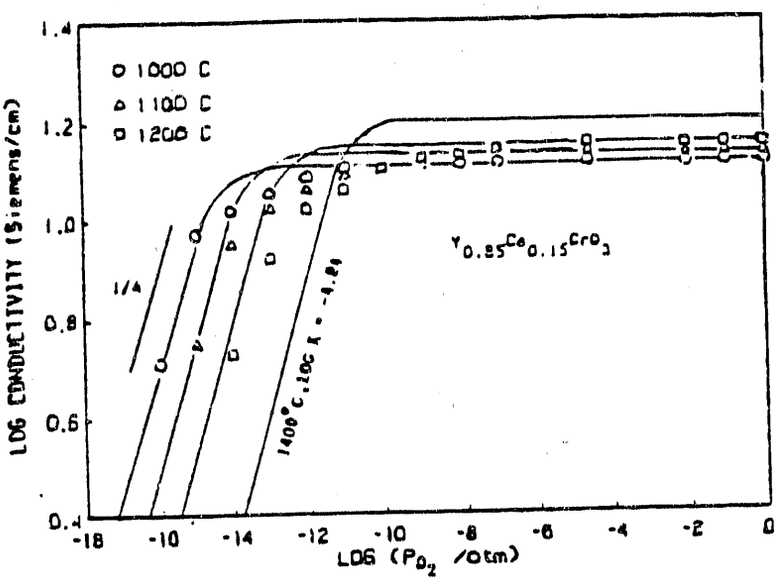

Figure 12a:

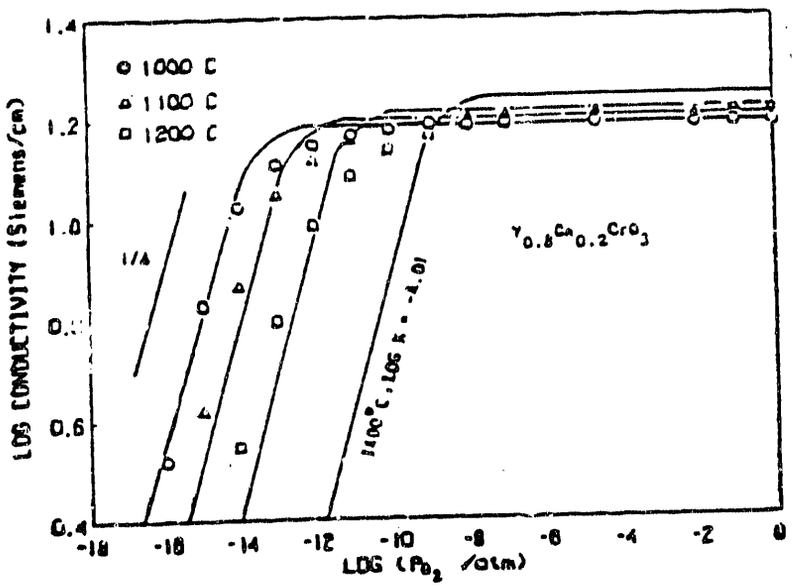

Figure 12b: Conductivity of $Y_{.80}Ca_{.20}CrO_3$ (12b) and $Y_{0.85}Ca_{0.15}CrO_3$ (12a) as function of temperature and oxygen activity

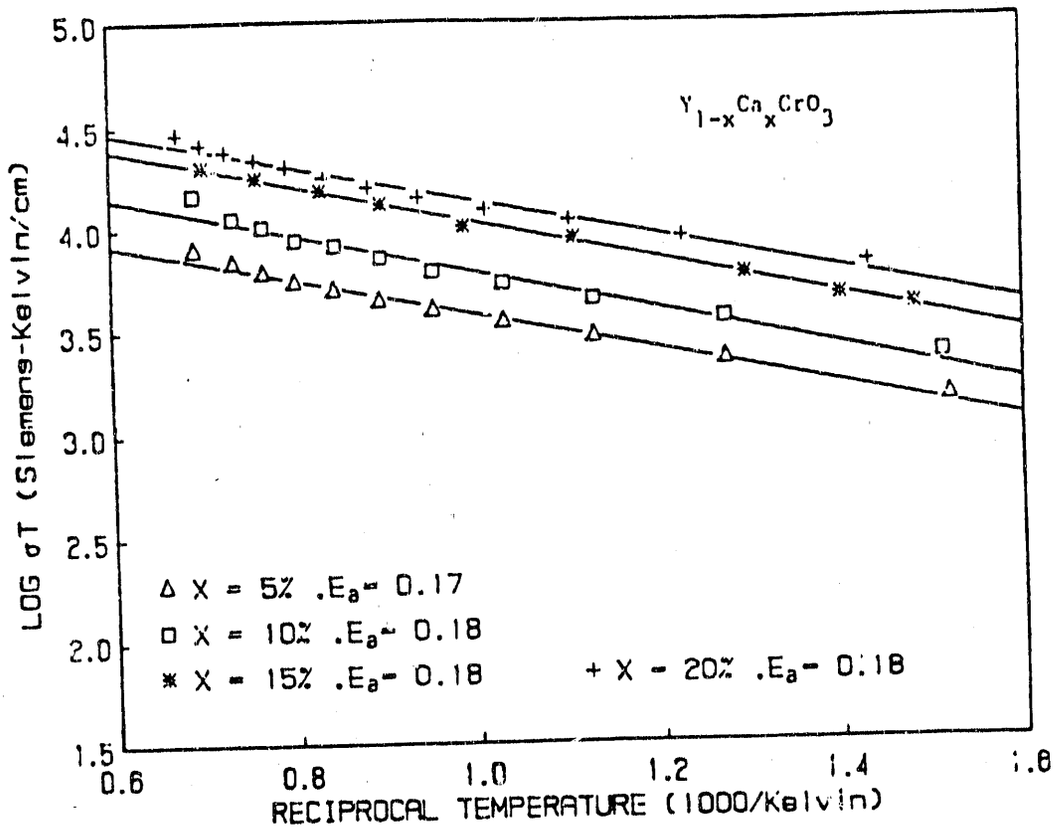

Figure 13: **Log σT vs. reciprocal temperature for various Ca-dopant levels. The solid lines are calculated by the least squares method**

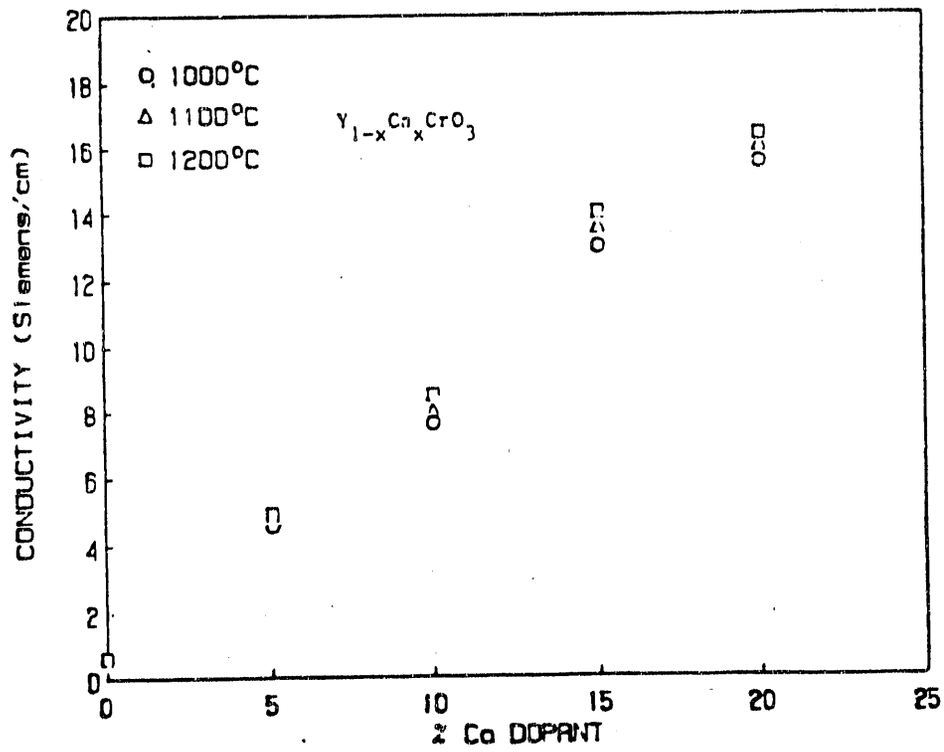

Figure 14: **Conductivity vs. Ca-dopant concentration at various temperatures**

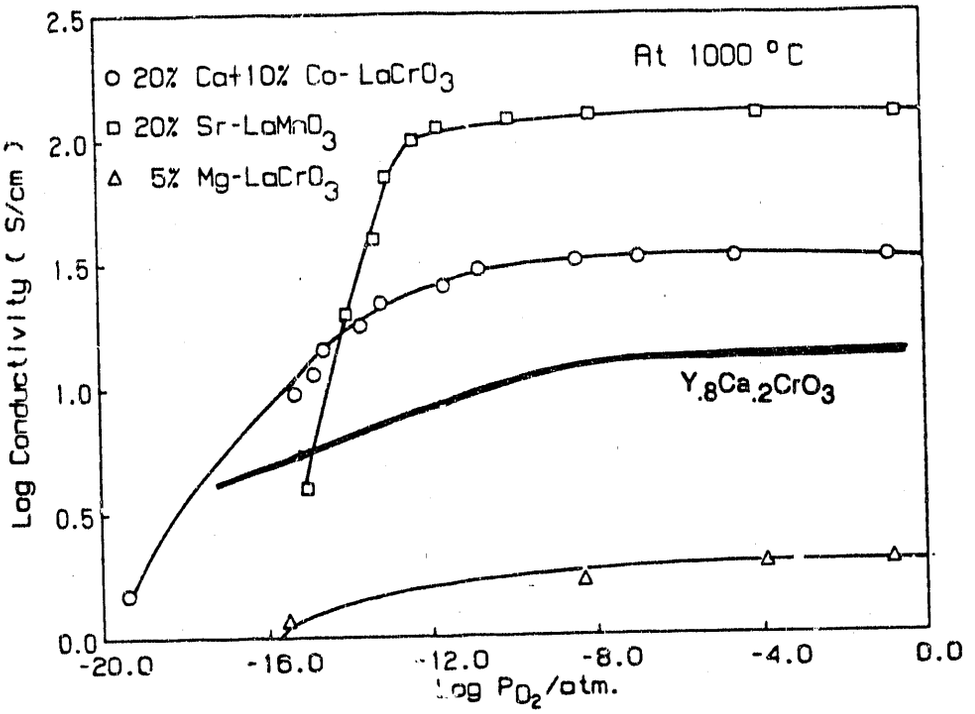

Figure 15: Comparison of electrical conductivity of $La_{.8}Ca_{.2}Cr_{.9}Co_{.1}O_3$, $La_{.8}Sr_{.2}MnO_3$ and $LaCr_{.95}Mn_{.05}O_3$ at 1000°C as function of oxygen activity

Preliminary a.c. conductivity measurements indicate that some compositions in this series have high electrical conductivity, as shown below:

Composition	Conductivity (S/cm)	Temp (C)
$Y_{.9}Ca_{.1}MnO_3$	13.4	920°
$Y_{.8}Ca_{.2}MnO_3$	56.0	925°
$Y_{.7}Ca_{.3}MnO_3$	87.6	935°
$Y_{.6}Ca_{.4}MnO_3$	133.2	907°
$Y_{.5}Ca_{.5}MnO_3$	167.3	926°

The following activation energies were calculated:

Composition	Activation Energy (eV)
$Y_{.9}Ca_{.1}MnO_3$	.26
$Y_{.8}Ca_{.2}MnO_3$	.26
$Y_{.7}Ca_{.3}MnO_3$	.19
$Y_{.6}Ca_{.4}MnO_3$	.14
$Y_{.5}Ca_{.5}MnO_3$	.10

As can be seen the electrical conductivity of $Y_{.6}Ca_{.4}MnO_3$ is as high as that of $La_{.8}Sr_{.2}MnO_3$. We know nothing regarding its stability towards reduction, but will be gathering that information soon.

C. $YCrO_3$ - $YMnO_3$ - $YCoO_3$ System

A survey of the electrical conductivity was made at 1000°C in air for the $YCrO_3$ - $YMnO_3$ - $YCoO_3$ system (figure 16). These data show that the maximum conductivities occur in the high Co and Mn concentration regions. However, since from other data we know that compositions containing more than 30 m% of either Co or Mn will be unstable towards reduction we focussed our attention to the $YCrO_3$ corner of the diagram. As a result we have made some Ca doped formulations in the composition range 50 to 60 m% Cr, 10 to 20 m% Ca and 10 to 20 m% Mn.

Figure 17 shows the electrical conductivity of compositions $Y_{.7}Ca_{.3}Cr_{.5}Mn_{.3}Co_{.2}O_3$ and $Y_{.7}Ca_{.3}Cr_{.6}Mn_{.2}Co_{.2}O_3$ at 900°C as function of oxygen activity. The data show that these compositions are both electrically and structurally nearly as stable as $LaCrO_3$ (See Figure 15). These results are very encouraging, but more work needs to be done to further define the best formutations (with electrical conductivity in air > 60 S/cm).

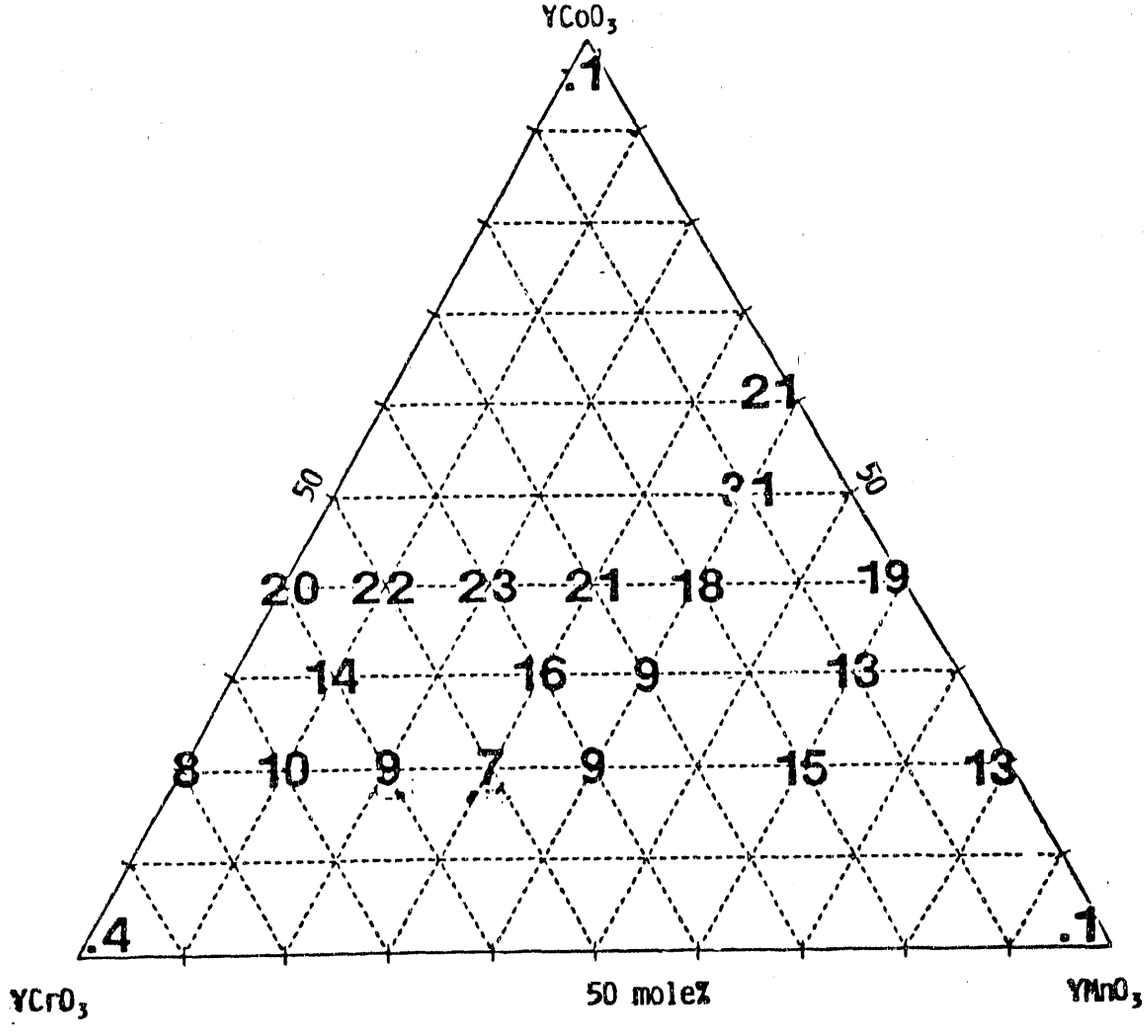

Figure 16: dc conductivity 1000° (S/cm)

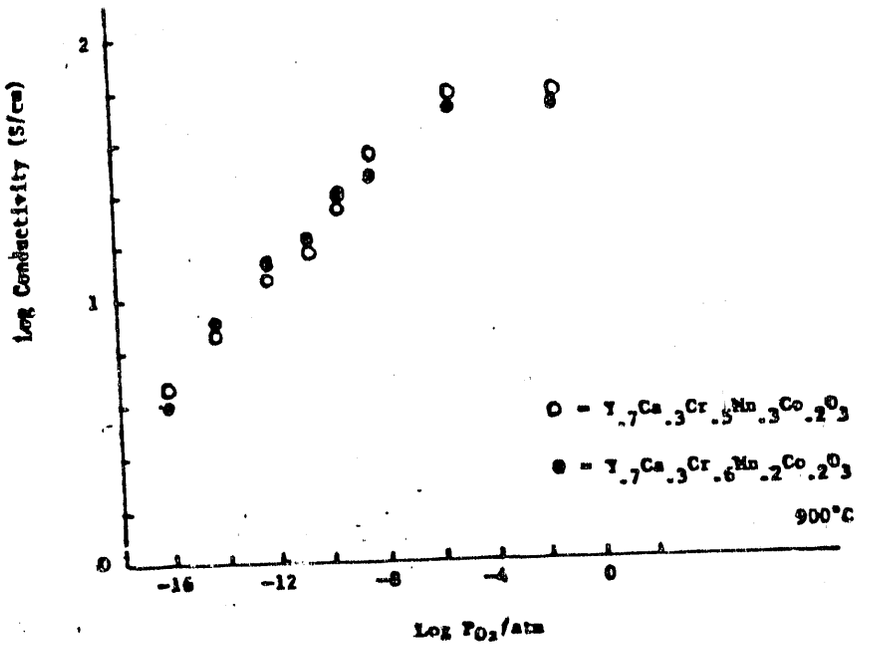

Figure 17: Electrical conductivity of $Y_{.7}Ca_{.3}Cr_{.5}Mn_{.3}Co_{.2}O_3$ and $Y_{.7}Ca_{.3}Cr_{.6}Mn_{.2}Co_{.2}O_3$ as function of oxygen activity at 900°C

III. Thermal Expansion Coefficient

All of the thermal expansion coefficient (TEC) data taken during the course of this program will be tabulated in this section. Although, we observe specific parameters that affect the TEC of various compounds upon doping, however, at the moment we offer no explanation for the trends.

A. $LaCrO_3$ - $LaCoO_3$ System

The thermal expansion coefficients were determined and given in Tables V and VI as a function of Co and Ca substitution. The TEC increased with increasing Co content. This must be due to the high thermal expansion coefficient of $LaCoO_3$ which was reported to be approximately 22 x 10^{-6}/°C. The TEC of compositions with y > 0.5 changed little with further increase in Co content and remained in the region of 20-23 x 10^{-6}/°C. However, when Co content was further decreased the TEC values decreased to 13.1 x 10^{-6}/°C at y = 0.1.

Additional Ca substitution for La decreased the TEC. The TEC of $La_{.7}Ca_{.3}Cr_{.9}Co_{.1}O_3$ had a value of 10.4 x 10^{-6}/°C. This value matches that of Y-PSZ. Therefore, the thermal expansion coefficient of the $LaCrO_3$ can be increased to match those of the other SOFC components by Co and Ca substitutions. The substitution of Ca for La in the $LaCr_{1-y}Co_yO_3$ resulted in formation of Cr^{4+} and Co^{4+} in order to maintain the electrical neutrality. Formation of both Cr^{4+} and Co^{4+} decrease the unit cell volume, since in these valence states

the radius of Cr^{4+} and Co^{4+} ions is markedly lower than that of Cr^{3+} and Co^{3+}. The decrease in TEC with increasing Ca content is probably associated with the formation of Cr^{4+} and Co^{4+} ions.

Table V. Thermal Expansion Coefficients as a Function of Co

$LaCr_{1-y}Co_yO_3$ (100-1100°C)

Composition (y)	TEC (10^{-6}/°C)
0.0	9.50
0.1	13.10
0.2	13.60
0.3	15.90
0.5	21.80
0.7	22.30
0.9	22.80
1.0	23.20

Table VI. Thermal Expansion Coefficients as a Function of Ca

$La_{1-x}Ca_xCr_{.9}Co_{.1}O_3$ (100 - 1100°C)

Composition (x)	TEC (10^{-6}/°C)
0.0	13.10
0.1	12.30
0.2	11.10
0.3	10.40

$La_{1-x}Ca_xCr_{.8}Co_{.2}O_3$ (100 - 1100°C)

Composition (x)	TEC (10^{-6}/°C)
0.0	13.60
0.1	13.40
0.2	11.50
0.3	10.40

B. $La_{.9}Sr_{.1}Cr_{1-x}Mn_xO_3$ System

Table VII shows the dependence of the thermal expansion coefficient on Mn content. As can be seen the TEC increases as the Mn content increases.

Table VII. Thermal Expansion $La_{.9}Sr_{.1}Cr_{1-x}Mn_xO_3$

Mn Content	TEC x 10^6C^{-1}
0 m%	10.7
10	9.6
20	10.0
30	9.5
40	10.0
50	10.5
60	10.1
70	10.4
80	11.8
90	11.5
100	11.6 - 12.0

C. $YCrO_3$ - $YCoO_3$ - $YMnO_3$

Figure 18 shows the room temperature X-ray diffraction analysis results. As can be seen most of the compositions are orthorhombic. We found it difficult to sinter compositions along the binary tie lines. The compositions in the ternary regions all tended to sinter well. We are now starting to add Ca, so we may find changes in the densification characteristics. Figure 19 shows the thermal expansion coefficient in this system.

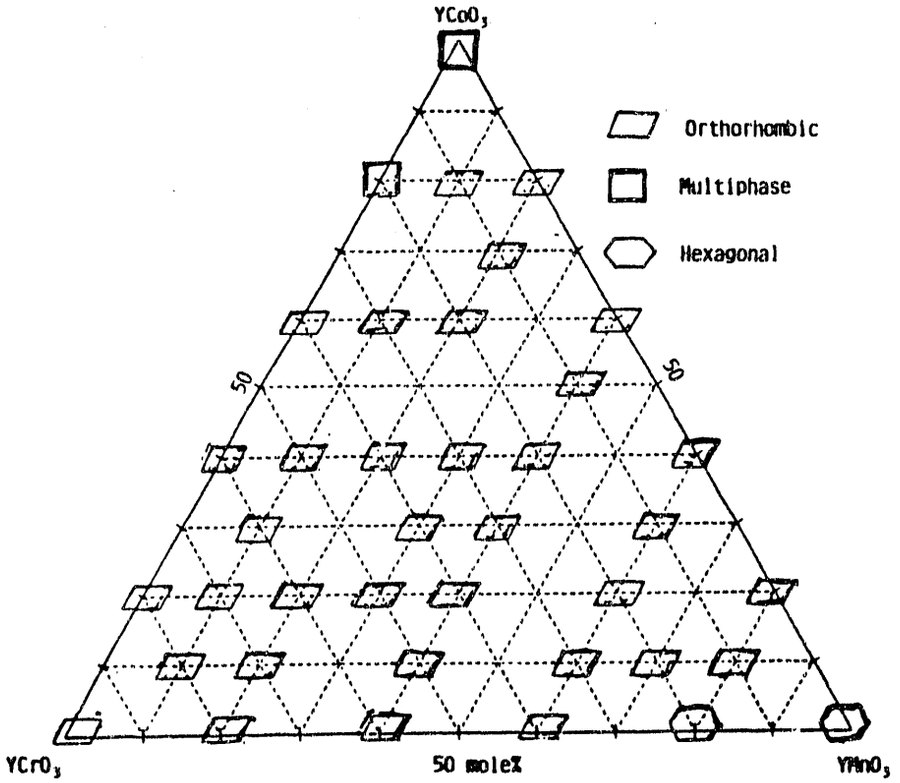

Figure 18: Crystal structure 1100°C

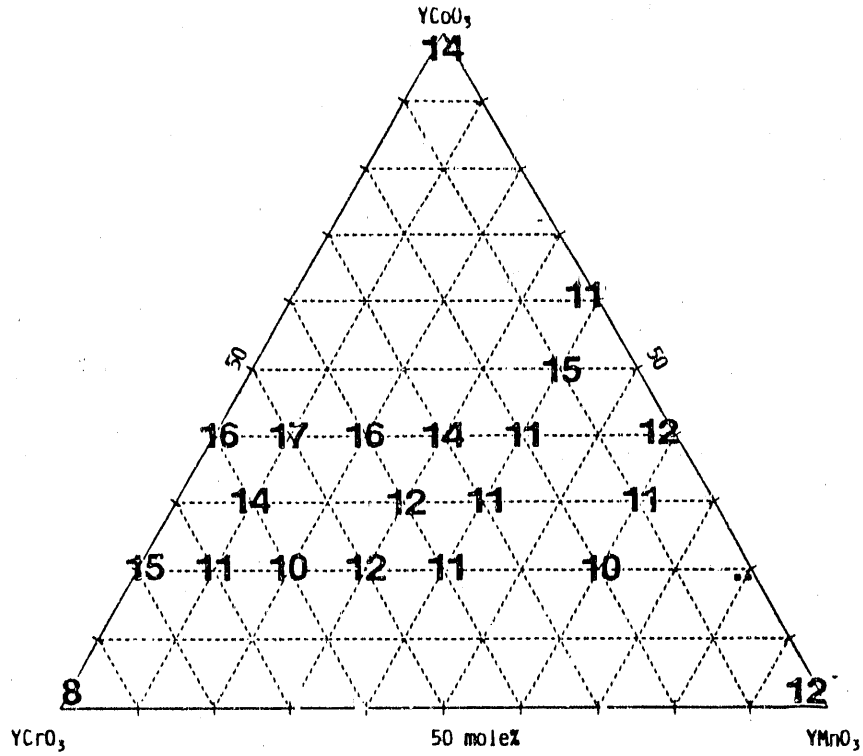

Figure 19: Thermal expansion 500-1000°C (α *10^{+6})

D. $LaCrO_3$

The thermal expansion of $LaCrO_3$ was measured as function of Sr and Mg content. These data are listed in Table VIII. The data show that Sr doping can yield a TEC match with Zirconia.

Table VIII. Thermal Expansion Coefficients of Ca, Mg and Sr-Doped $La_{.99}CrO_3$

Compounds	Thermal Expansion Coefficient (x 10^{-6}/°C)
$La_{.99}CrO_3$	9.4
$La_{.99}Cr_{.98}Mg_{.02}O_3$	9.4
$La_{.99}Cr_{.95}Mg_{.05}O_3$	9.5
$La_{.99}Cr_{.90}Mg_{.10}O_3$	9.4
$La_{.99}Cr_{.85}Mg_{.15}O_3$	9.5
$La_{.97}Sr_{.02}CrO_3$	10.2
$La_{.94}Sr_{.05}CrO_3$	10.8
$La_{.89}Sr_{.10}CrO_3$	10.7
$La_{.84}Sr_{.15}CrO_3$	10.8
$La_{.79}Sr_{.20}CrO_3$	11.1
$La_{.89}Sr_{.10}CrO_3$	10.0

* Temperature range from 350 to 1000°C.

E. $LaMnO_3$

The thermal expansion of $LaMnO_3$ was measured as function of Sr content (Table IX). As can be seen, the TEC is greater than that of zirconia for all compositions.

Table IX.

Composition	$\alpha \times 10^6/°C$
$La_{.99}MnO_3$	11.2 ± 0.3
$La_{.94}Sr_{.05}MnO_3$	11.7
$La_{.89}Sr_{.10}MnO_3$	12.0
$La_{.79}Sr_{.20}MnO_3$	12.4
$La_{.69}Sr_{.30}MnO_3$	12.8

F. $YCrO_3$

The thermal expansion of $YCrO_3$ was measured as function of Ca content (fig. 20). Although Ca doping increased the TEC of $YCrO_3$, however, at the solubility limit of Ca in $YCrO_3$ the TEC is less than that of zirconia.

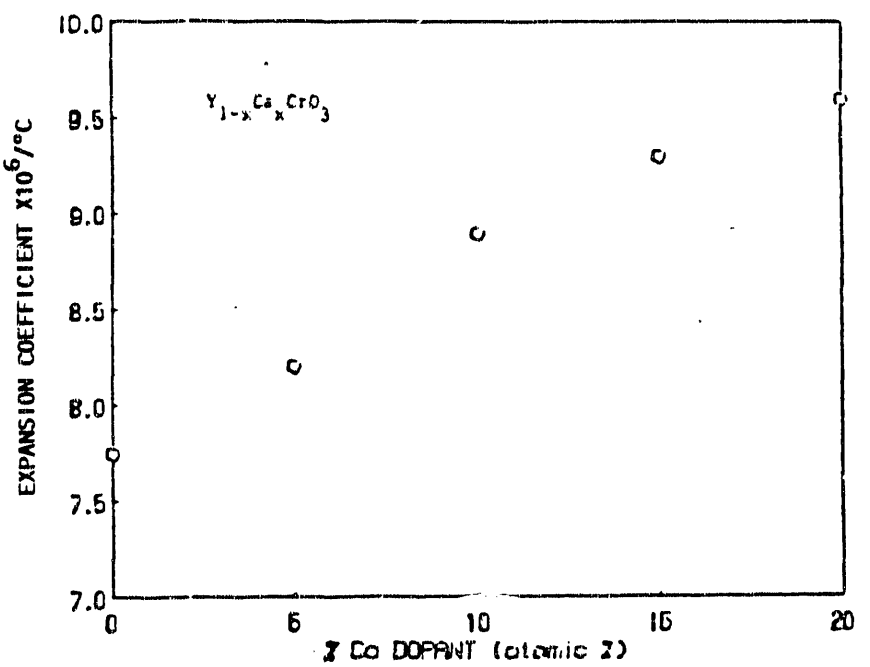

Figure 20.

IV. Films of $La_{.7}Ca_{.3}Cr_{1-x}Co_xO_3$ on Stabilized ZrO_2 Substrates

Inks were prepared of powders of composition $La_{.7}Ca_{.3}Cr_{.8-.95}Co_{.05-.2}O_3$ and either printed or painted onto dense ZrO_2 plates. Good adhesion and sintering was observed after

heat treatment in the 1300 to 1400°C range. Porosity appears to be controllable so that such coatings can be used as a cathode.

The sintering study showed that the optimum temperature range is 1300 to 1350°. Figure 21 is a SEM of $La_{.7}Ca_{.3}Cr_{.9}Co_{.1}O_3$ sintered on a YSZ substrate at 1350°C for 2 hours. This film is well sintered and as shown in Figure 22 is well bonded to the YSZ substrate. Figure 23 shows the same ink sintered at 1400°C for 2 hours. This film is quite dense and well sintered but the porosity is too low for use as a cathode for SOFC. At 1350°C, it appears that with a few adjustments in the ink, a porosity can be obtained that will allow the film to serve as a cathode for SOFC's.

In the future we will be attempting to optimize our inks and make some electrical conductivity measurements of the films.

We have also demonstrated our ability[16,17] to make films of $La_{1-x}Sr_xMnO_3$ on YSZ substrates. Dense (0.3 μm) as well as porous (5-25 μm) films were developed.

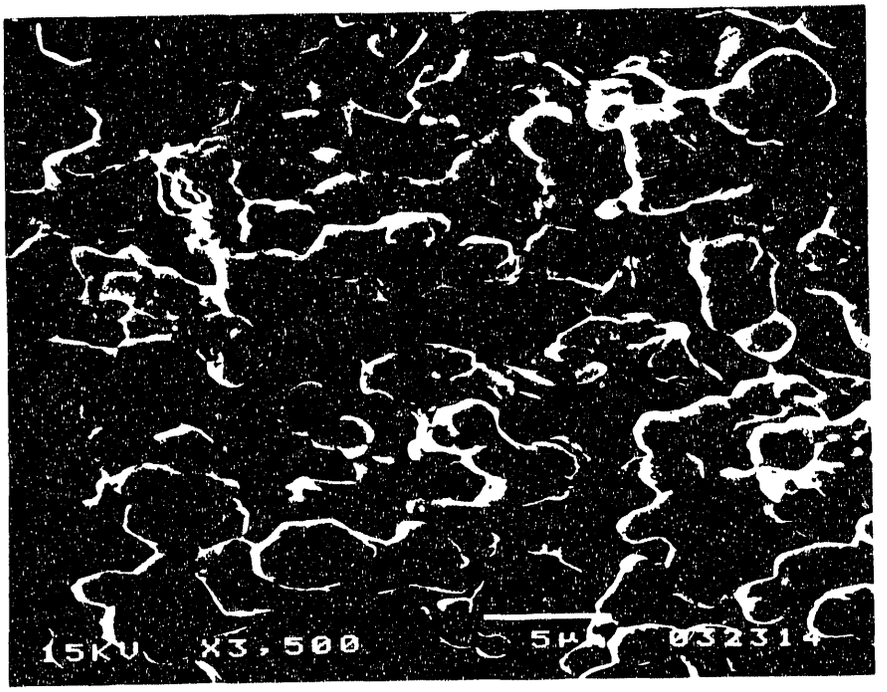

Figure 21: SEM Photomicrograph of Surface of a $La_{.7}Ca_{.3}Cr_{.9}Co_{.1}O_3$ Film on YSZ. T = 1350°C/2hr.

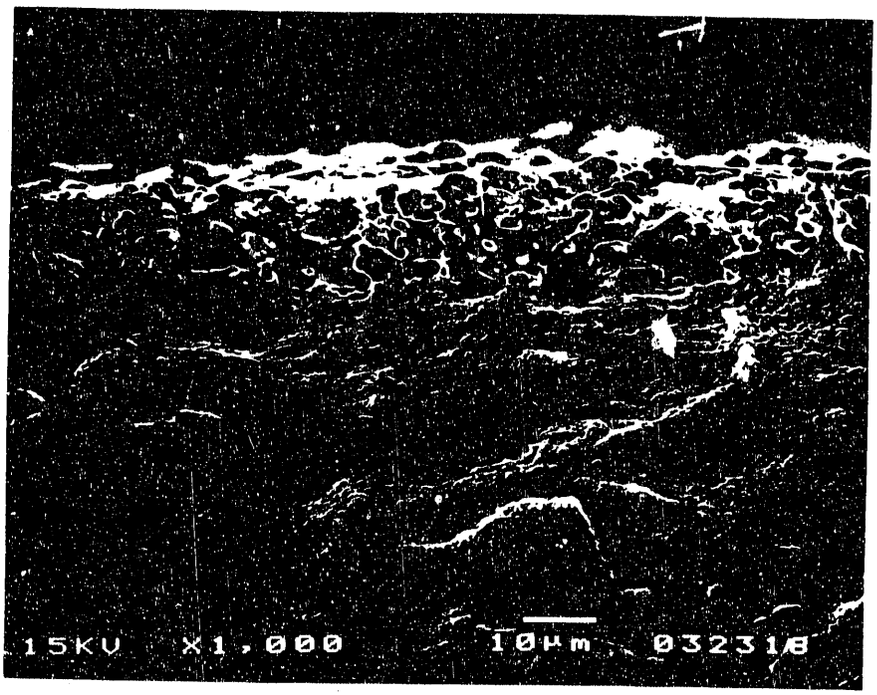

Figure 22: Scanning Electron Microscope Photomicrograph of Fracture Surface of a $La_{.7}Ca_{.3}Cr_{.9}Co_{.1}O_3$ Film on YSZ, T = 1350°C/2hr, Thickness ≅ 20-25µm.

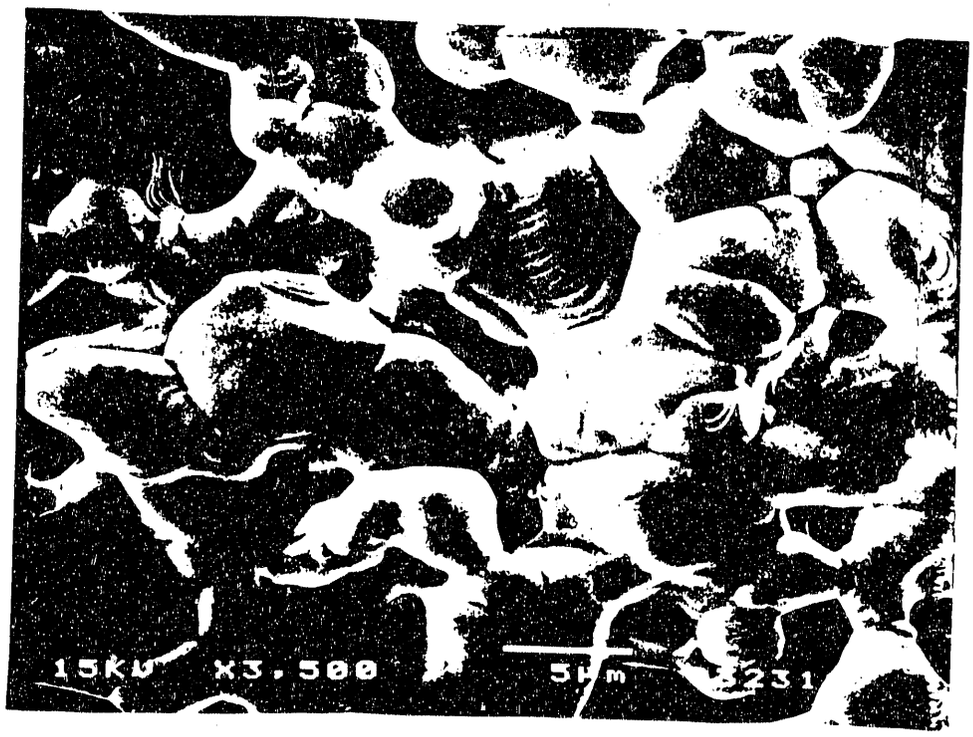

Figure 23a: SEM Photomicrograph of Surface of a $La_{.7}Ca_{.3}Cr_{.9}Co_{.1}O_3$ Film on YSZ, T = 1400°C/2hr.

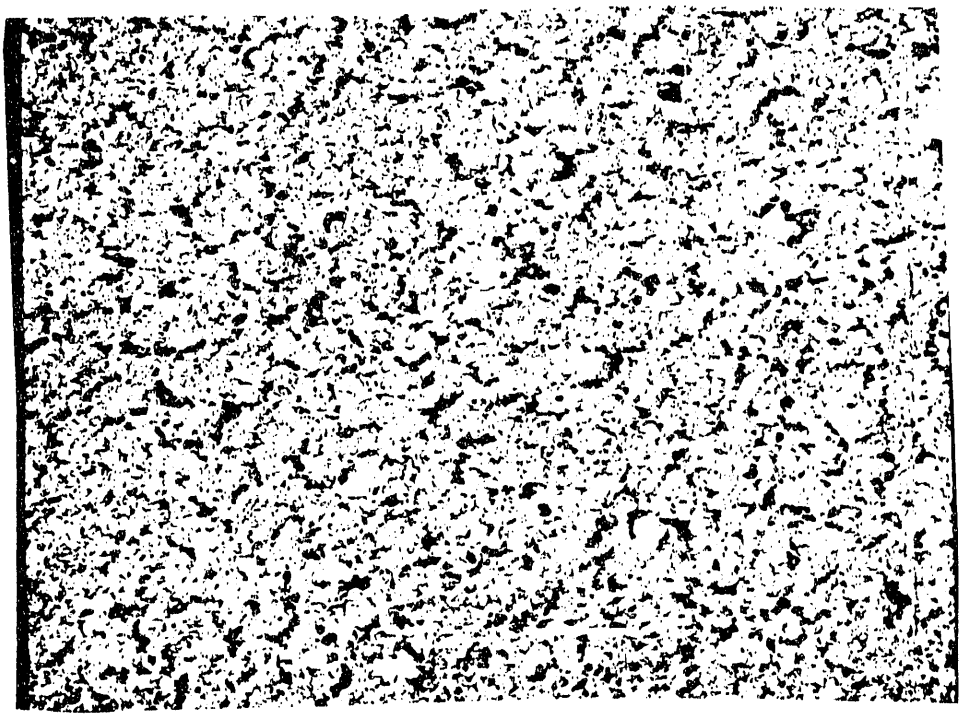

Figure 23b: SEM Photomicrograph of Surface of a $La_{.7}Ca_{.3}Cr_{.9}Co_{.1}O_3$ Film on YSZ, T = 1400°C/2hr.

4. Accomplishments and Conclusions

Although the entire time frame of this program was only 16 months, yet significant progress has been made towards the development of improved cathode materials. The highlights of our accomplishments include:

1. The results are very encouraging since the stability towards reduction in fuel gas is improved, and electrical conductivity of 60 S/cm at 1000°C is achieved. Thus, we have developed a system which does not reduce in fuel gas, and has a conductivity within 50% of that of $La_{.8}Sr_{.2}MnO_3$.
2. We have prepared 1Kg quantities of a potential composition for cathode applications ($La_{.79}Ca_{.2}Cr_{.9}Co_{.1}O_3$) and delivered them to AirResearch and Westinghouse for evaluations as per our program commitment.
3. We have shown that the $La_{1-x}Ca_xCr_{1-y}Co_yO_3$ system has thermal expansion coefficients ranging from 10.5×10^{-6}/°C to 11.5×10^{-6}/°C.
4. $La_{.7}Ca_{.3}Cr_{1-x}Co_xO_3$ powders were sintered onto YSZ plates. Good adhesion and sintering were observed upon heat treatment in the 1300° to 1400°C range with X = 0.05%. The porosity appears to be controllable so that such coatings can be used as cathodes.

5. The stability of $Y_{.7}Ca_{.3}Cr_{.5}Mn_{.3}Co_{.2}O_3$ and $Y_{.7}Ca_{.3}Cr_{.6}Mn_{.2}Co_{.2}O_3$ towards reduction was evaluated at 900°C. The results show that these compositions are quite stable and are potential candidates for cathode applications. Work should continue in this area.

6. We have started our reduction stability studies of the $YCrO_3$-$YMnO_3$-$YCoO_3$ system. Our results to date suggest that this system may yield a good cathode material. Work should be continued here. It is encouraging to realize that $Y_{.6}Ca_{.4}MnO_3$ has conductivities comparable to those of $La_{.8}Sr_{.2}MnO_3$. We plan to complete these studies but not during our contract period. Our focus will be on compositions with high Cr content in this system.

7. Our results suggest that we need to continue our investigation on the effect of multiple substitution on both the A and B lattice site of $LaCrO_3$ with cations which have variable valences as we suggested in our proposal. We have done some of this, however, we did not complete this task within the contract period. This is probably the only method by which we can increase the hole mobility in $LaCrO_3$ sufficiently for cathode applications. This is a good area for future studies.

8. Our efforts within the frame work and duration of this project resulted in several publications and presentations in international meetings. These were supported either fully or in part by this program. A list is shown in section 7.

5. References

1. G. Carini II, "An Apparatus for the Measurement of dc Electrica Conductivity and Seebeck Coefficient of Semiconductors as a Function of High Temperature and Oxygen Partial Pressure", M.S. Thesis, University of Missouri-Rolla, 1987.
2. M.P. Pechini, "Method of Preparing Lead and Alkaline Earth Titanates and Niobates and Coating Method Using the Same to From a Capacitor", U.S. Patent No. 3,330,697, July 1967.
3. L. Groupp and H.U. Anderson, "The Influence of Oxygen Activity on Sintering of Sr-Doped Lanthanum Chromite", J. of Amer. Cer. Soc., 59, 449-53, 1976.
4. D.B. Meadowcroft, "Some Properties and Application of Strontium-Doped Rare- Earth Perovskites", Proceeding of the Conference on Sr Containing Compounds, 118-35, 1973.
5. B.K. Flandermeyer, R.B. Poeppel, J.T. Dusek and H.U. Anderson, "Sintering Aid For Lanthanum Chromite Refractories", U.S. Patent #4,749,632, 1988.

6. D.P. Karim and A.T. Aldred, "Localized Level Hopping Transport in La(Sr)CrO_3", Phys. Rev. B, 20, 6, 2255-63, 1979.

7. S. Song, M. Yoshimura and S. Somiya, "Hydrothermal Synthesis of $(La_{1-x}Ca_x)CrO_3$", J. Mater. Sci. Soc. Jpn., 19, No. 1, 49, 1982.

8. P.M. Raccah and J.B. Goodenough, "First-Order Localized-Electron Versus Collective Electron Transition in $LaCoO_3$", Phys. Rev. 155, 932, 1967.

9. H. Taguchi, M. Shimada and M. Koizumi, "Electrical Properties in the System $(La_{1-x}Ca_x)CoO_3$ $(0.1<x<0.5)$", J. of Solid State Chemistry, 44, 254-56, 1982.

10. P.M. Raccah and J.B. Goodenough, "A Localized-Electron to Collective-Electron Transition in the System $(La,Sr)CoO_3$", J. of Appl. Phys., 39, 2, 1209-12, 1968.

11. H. Ohbayashi, T. Kudo and T. Gejo, "Crystallographic, Electric and Thermochemical Properties of the Perovskite-Type $In_{1-x}Sr_xCoO_3$ (Ln: Lanthanoid)", J. of Appl. Phys., 13, 1, 1-7, 1974.

12. J.F. Kononyuk, S.P. Tolochko, V.A. Lutsko and V.M. Anishchic, "Preparation and Properties of $La_{1-x}Ca_xCoO_3$ $(0.2<x<0.6)$", J. of Solid State Chemistry, 48, 209-14, 1983.

13. F.R. Van Buren and J.H.W. de Wit, "The Thermoelectric Power of $La_{1-x}Sr_xCoO_{3-y}$", J. Electrochem. Soc., 126, 1817-20, 1979.

14. B.K. Flandermeyer, M.M. Nasrallah, A.K. Agarwal and H.U. Anderson, "Defect Structure of Mg-Doped $LaCrO_3$: Model and Thermogravimetric Measurements", J. Am. Cer. Soc., 67, 195, 1984.

15. F.A. Kroger and H.J. Vink, "Solid State Physics", Vol. 3, Ed., by F. Seitz and D. Turnbull, Academic Press, New York, 307, 1965.

16. H.U. Anderson, C.C. Chen and J.C. Wang, "Synthesis of Conducting Oxide Films and Powders from Polymeric Precursors", Ceramic Powder processing Sc. III, Ed. G. Messing, H. Hausner and S. Hirano, Amer. Cer. Soc., 1990.

17. H.U. Anderson, M.M. Nasrallah, F. Blum and M. Smith, "Polymeric Synthesis of Perovskite Powders and Films", Proc. Intl. Conf. on the Chemistry of Electronic Ceramic Materials, NIST SP 804, 1991.

6. Contributors to Program

1. Dr. H.U. Anderson, Curators' Professor of Ceramic Engineering and Senior Investigator, Materials Research Center, Principal Investigator and Program Director.

2. Dr. Magdi M. Nasrallah, Research Professor and Co-Principal Investigator. His responsibilities include assistance with experimental details and guidance in interpretation of results.
3. Dr. Rasit Koc obtained his Ph.D. in Dec. 1989, and was supported in part by this program. He studied the stability and sintering of compositions in the $LaCrO_3$-$LaMnO_3$ -$LaCoO_3$ system.
4. Dr. G. Carini obtained his Ph.D. in Dec. 1990, and was supported by other funds. He studied the effect of cation stoichiometry and dopants on the $YCrO_3$-$YMnO_3$ system.
5. J.D. Carter, Ph.D. candidate, supported by other funds. He is studying the mechanism of low temperature sintering and properties of the $Y_{1-x}Ca_xCr_{1-y}Co_yO_3$ system.
6. J.W. Stevenson, Ph.D. candidate and supported by other funds. He is investigating the electrical and thermal characteristics of the $Y_{1-x}Ca_xMnO_3$ system.

7. Manuscripts Published or Presented

1. "Thermal Expansion Studied on Cathode and Interconnect Oxides", S. Srilomsak, D.P. Schilling and H.U. Anderson, Proc. of First Intl. Symp. on Solid Oxide Fuel Cells, Ed. S. Singhal, Electrochem. Soc., (1989).
2. "Review of Defect Chemistry of $LaMnO_3$ and $LaCrO_3$", H.U. Anderson, J.H. Kuo and D.M. Sparlin, Proc. of First Intl. Symp. on Solid Oxide Fuel Cells, Ed. S. Singhal, Electrochem. Soc., (1989).
3. S. Seward, G. Carini and H.U. Anderson, "Structural, Sintering and Electrical Properties of the $YCrO_3$-$YMnO_3$-$YCoO_3$", First Intl. Symp. on Solid Oxide Fuel Cells, Ed. S. Singhal, Electrochem. Soc., Hollywood, FL, Oct. 1989.
4. R. Koc and H.U. Anderson, "$LaCrO_3$ Based Ceramics", First Intl. Symp. on Solid Oxide Fuel Cells, Ed. S. Singhal, Electrochem. Soc., Hollywood, FL, Oct. 1989.
5. R. Koc, H.U. Anderson and M.M. Nasrallah, "Effects of Processing and Dopants on Air Sinterable $LaCrO_3$", Am. Ceram. Soc., Dallas, TX, April 1990.
6. R. Raffaelle, H.U. Anderson, D.M. Sparlin and P.E. Parris, "Transport Anomalies in the High Temperature Hopping Conductivity and Thermoelectric Power of Sr-doped $La(Cr,Mn)O_3$", submitted to Physical Rev. B., August 1990.
7. R. Koc and H.U. Anderson, "Low Temperature Sintering of $YCrO_3$ and $LaCrO_3$ Based Ceramics", Ceramic Powder Processing Science III, Ed. G. Messing, H. Hausner & S. Hirano, Amer. Cer. Soc., 1990.

8. H.U. Anderson, C.C. Chen, J.C. Wang and M.J. Pennell, "Synthesis of Conducting Oxide Films and Powders from Polymeric Precursors", Ceramic Powder Processing Science III, ibid.

9. H.U. Anderson, M.M. Nasrallah, F. Blum and M. Smith, "Polymeric Synthesis of Perovskite Powders and Films", Proc. Intl. Conf. on the Chemistry of Electronic Ceramic Materials, Grand Teton, WY, August 1990.

10. H.U. Anderson, M.M. Nasrallah, R. Koc and D. Carter, "Air Sinterable Solid Oxide Fuel Cell Interconnects", 1990 Fuel Cell Seminar, Phoenix, AZ, November 25-28, 1990.

11. G.F. Carini, H.U. Anderson, D.M. Sparlin and M.M Nasrallah, "Electrical Conductivity, Seebeck Coefficient and Defect Chemistry of Ca-doped $YCrO_3$", Accepted for publication, Solid State Ionics.

12. G.F. Carini, H.U. Anderson, M.M. Nasrallah and D.M. Sparlin, "Defect Structure, Nonstoichiometry and Phase Stability of $Y_{1-x}Ca_xCrO_3$", Submitted, J. Solid State Chem.

13. J.W. Stevenson, M.M. Nasrallah and H.U. Anderson, "Electrical and Structural Characteristics of $Y_{1-x}Ca_xMnO_3$", ibid.

14. D.C. Carter, M.M. Nasrallah and H.U. Anderson, "Properties of Liquid Phase Sintered $LaCrO_3$ and $YCrO_3$", Ceramic Society Meeting, Cincinnati, OH, April 1991.

15. H.U. Anderson and G. Carini, "Defect Chemistry and Properties of $Y_{1-x}Ca_xCrO_3$", 6th Workshop on Nonstoichiometric Compounds, Tokyo, Japan, December 3-5, 1990.

16. M.M. Nasrallah, H.U. Anderson and J.W. Stevenson, "Defect Chemistry and Properties of $Y_{1-x}Ca_xMnO_3$", 2nd International Symposium on Solid Oxide Fuel Cells, Athens, Greece, July 2-5, 1991.

17. M.M. Nasrallah, D.C. Carter and H.U. Anderson, "Low Temperature Air-Sinterable $LaCrO_3$ and $YCrO_3$", ibid.

END

DATE FILMED

8/28/92